Paper ID APEN-MIT-2020_84
Applied Energy Symposium: MIT A+B
May 17-19, 2020 • Cambridge, USA

Performance of a modified two-phase thermofluidic oscillator with low GWP working fluids for low-grade waste heat recovery

Jingqi Tan
Institute of Refrigeration and Cryogenics
Zhejiang University
Hangzhou, China
11627050@zju.edu.cn

Jiaqi Luo
Institute of Refrigeration and Cryogenics
Zhejiang University
Hangzhou, China
11827052@zju.edu.cn

Jianjian Wei
Institute of Refrigeration and Cryogenics
Zhejiang University
Hangzhou, China
weijzju@zju.edu.cn

Tao Jin
Institute of Refrigeration and Cryogenics
Zhejiang University
Hangzhou, China
jintao@zju.edu.cn

Abstract—Two-phase thermofluidic oscillator has attracted considerable attention for low-grade heat recovery, thanks to its ability to operate across a small temperature difference between heat source and sink. The performance of a modified two-phase thermofluidic oscillator with the working fluids of low global warming potential (e.g., R152a, R1234yf and R1234ze(E)) for harvesting low-grade waste heat is investigated. An acoustic-electric analogy model is proposed for predicting the onset temperature difference and oscillation frequency, which is then verified by experiments. The model can well predict the oscillation frequency, with the differences of 4.4-6.8% from experimental data. The predicted and measured onset temperature differences are also in reasonable agreement, for the model underestimates by 5.4-13.4% compared with the experimental results. The influences of the lengths and diameters of feedback connection tube and vapor connection tube on the performance are also numerically studied. A lowest onset temperature difference of 14.4°C can be obtained with the vapor connection tube diameter of 0.015 m and the working fluid of R1234yf. In addition, a highest oscillation frequency achieved is 3.04 Hz with R152a as working fluid, when the feedback connection tube diameter is increased to 0.019 m. This work verifies the feasibility of recovering low-grade waste heat to drive a two-phase thermofluidic oscillator with the low global warming potential working fluids.

Keywords—two-phase thermofluidic oscillator, low global warming potential, low-grade heat, acoustic-electric analogy, oscillation frequency, onset temperature difference

I. Introduction

Global warming is recognized as one of the most serious environmental problems in the world. In 2018, the Intergovernmental Panel on Climate Change announced that the global mean surface temperature has warmed up by approximately 0.87°C since the industrial age [1]. The reduction of carbon emission, especially in energy conversion processes, is significant for mitigating global climate change [1]. Utilization of low-grade waste heat (in the form of compressed air, high temperature flue gases and cooling water) can improve the energy efficiency, thereby reducing global energy consumption and carbon emission [2].

Recently, much interest has been drawn on low-grade waste heat recovery. Among the available technologies such as organic Rankine cycle [2], Kalina cycle [3] and thermoacoustic engine [4], two-phase thermofluidic oscillator [5] has received increasing attention, thanks to its ability to operate across a small temperature difference between heat source and sink. In 2004, Smith [5] constructed a two-phase non-inertive-feedback thermofluidic engine (NIFTE), which was featured as having no moving parts. The lowest onset temperature was only 50℃ with *n*-pentane as working fluid, suitable to utilize low-grade waste heat. Taleb et al. [6] proposed an evaporative reciprocating piston engine (ERPE), which could covert waste heat to positive displacement work through the vapor-liquid phase change of working fluid. Later, another two-phase single reciprocating piston thermofluidic oscillator termed Up-THERM was built by Glushenkov et al. [7] and further developed by Kirmse et al. [8]. The electric power could be generated by adopting a pair of hydraulic accumulators and check valves, which provided inspiring availability in the combined heat and power (CHP) system.

Our previous work [9, 10] proposed a modified two-phase thermofluidic oscillator, where a screen-stacked regenerator was introduced for reducing the irreversible loss induced by heat transfer. An onset temperature difference as low as 8.2℃ was obtained when adopting R134a as working fluid, showing good applicability to low-grade thermal energy. However, R134a, as a hydrofluorocarbon refrigerant, has a high global warming potential (GWP) of 1300, and thus contributes greatly to the global warming. The United States Environmental Protection Agency (USEPA) declared that hydrofluorocarbon refrigerants such as R134a and

R143a would no longer be adopted from 2024 [10]. In order to alleviate the environmental pressure, there is an urgent need to use the alternatives with zero ozone depletion potential (ODP) and low GWP as working fluids in the two-phase thermofluidic oscillator.

In this work, the applicability of low GWP working fluids for a modified two-phase thermofluidic oscillator with regenerator is investigated. Three working fluids studied are R152a, R1234yf and R1234ze(E). An acoustic-electric analogy model is established for predicting onset temperature difference and operating frequency. The results are validated by experiments. The influences of the lengths and diameters of feedback connection tube and vapor connection tube on the performance are then numerically investigated.

II. Experimental System

A. *Configuration of two-phase thermofluidic oscillator*

Fig. 1 schematically illustrates a modified two-phase thermofluidic oscillator, which contains a looped structure, a gas reservoir and a load tube. The looped structure contains a hot heat exchanger, a cold heat exchanger, a regenerator, a displacer cylinder, a power cylinder, a vapor connection tube and a feedback connection tube. Different from the NITFE [5], a regenerator stacked with 120-mesh stainless steel screens is added for reducing the irreversible loss induced by heat transfer. In addition, a gas reservoir is introduced for forming a closed system, while simultaneously creating the local travelling-wave phasing in the regenerator. Dimensions of main components in the thermofluidic oscillator are listed in Table I. The volume of gas reservoir is 0.0015 m^3.

B. *Measurement and error analysis*

As depicted in Fig. 1, two pressure sensors (GE UNIK 5000), with the accuracies of 0.2% FS, are installed to monitor the pressure oscillations, whose signals are acquired by an analog input module (NI 9205). Four thermometers (CHINO PT100), with the accuracies of ±0.1°C, are installed to monitor the hot and cold temperatures, whose signals are then acquired by an analog input module (NI 9217). In addition, the input power is measured by an electric power meter (WEIBO 1200).

The measurement error σ_m is divided into two parts [11]:

$$\sigma_{\mathrm{m}} = \sqrt{\sigma_{\mathrm{s}}^2 + \sigma_{\mathrm{r}}^2} \tag{1}$$

where the systematic error σ_s depends on the measurement accuracy of instrument and the random error σ_r is estimated by [11]:

$$\sigma_{\mathrm{r}} = \sqrt{\frac{\sum_{i=1}^{n}\left(x_{\mathrm{i}} - \overline{x_{\mathrm{i}}}\right)^2}{n-1}} \tag{2}$$

where n stands for the times of measurement and x_i represents the ith measured value. The uncertainties of frequency and temperature are in the range of ±0.008 Hz and ±0.38°C, respectively.

III. Acoustic-Electric Analogy Model

Based on the acoustic-electric analogy [12], the two-phase thermofluidic oscillator can be analogous to the AC current circuit, as depicted in Fig. 2. The two-phase heat transfer process in the regenerator of the modified two-phase thermofluidic oscillator is similar to that in a wet thermoacoustic engine, and then can also be analyzed with the wet thermoacoustic theory [13]. The wave equation for the first-order pressure amplitude in the regenerator could be expressed as follows [13]:

$$\left(1+(\gamma-1)f_\kappa+\frac{n_{\mathrm{w}}}{n_{\mathrm{g}}}\gamma f_D\right)p_1+\frac{\gamma p_{\mathrm{m}}}{\omega^2}\frac{d}{dx}\left(\frac{1-f_\nu}{\rho_{\mathrm{m}}}\frac{dp_1}{dx}\right) -\frac{a^2}{\omega^2}\left(\frac{f_\kappa-f_\nu}{1-\mathrm{Pr}}+\frac{l}{R_0T_{\mathrm{m}}}\frac{n_{\mathrm{w}}}{n_{\mathrm{g}}}\frac{f_D-f_\nu}{(1-\mathrm{Sc})}\right)\frac{1}{T_{\mathrm{m}}}\frac{dT_{\mathrm{m}}}{dx}\frac{dp_1}{dx}=0 \tag{3}$$

Equation (3) can be rewritten into two first-order equations for oscillating pressure and oscillating volume flow rate:

$$\Delta p_{\mathrm{r}} = -\frac{i\omega\rho_{\mathrm{m}}l_{\mathrm{r}}/A_{\mathrm{r}}}{1-f_\nu}U_{\mathrm{r}} \tag{4}$$

$$\Delta U_{\mathrm{r}} = -\frac{i\omega A_{\mathrm{r}}l_{\mathrm{r}}}{\gamma P_{\mathrm{m}}}[1+(\gamma-1)f_\kappa+\frac{n_{\mathrm{w}}}{n_{\mathrm{g}}}\gamma f_D]p_{\mathrm{r}} +\left\{\frac{(f_\kappa-f_\nu)}{(1-f_\nu)(1-\mathrm{Pr})}+\frac{l}{R_0T_{\mathrm{m}}}\frac{n_{\mathrm{w}}}{n_{\mathrm{g}}}\frac{(f_D-f_\nu)}{(1-f_\nu)(1-\mathrm{Sc})}\right\}\frac{dT_{\mathrm{m}}}{T_{\mathrm{m}}}U_{\mathrm{r}} \tag{5}$$

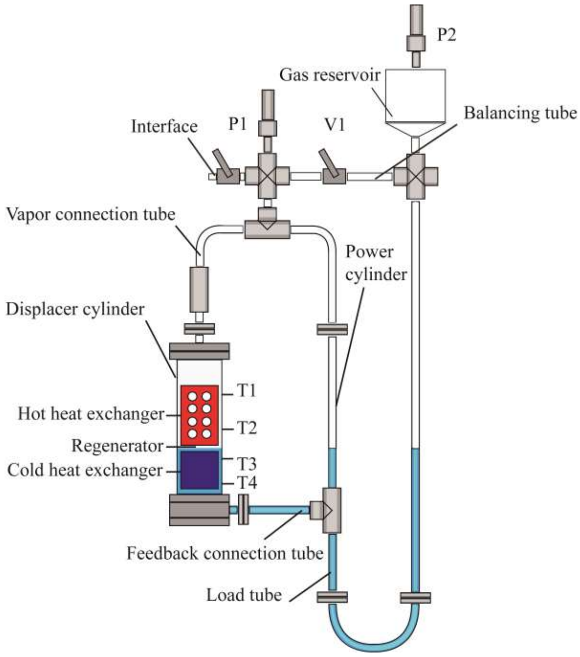

Fig. 1. Schematics of the modified two-phase thermofluidic oscillator.

TABLE I. Dimensions of Main Components in the Modified Two-Phase Thermofluidic Oscillator

Components	Diameter (m)	Length (m)	Hydraulic radius	Volumetric porosity
Regenerator (120-mesh)	0.056	0.005	0.0000499	0.740
Hot heat exchanger	0.056	0.064	0.00075	0.331
Cold heat exchanger	0.056	0.064	0.0005	0.551
Displacer cylinder	0.056	0.39	0.014	1
Power cylinder	0.017	0.39	0.00425	1
Feedback connection tube	0.017	0.15	0.00425	1
Vapor connection tube	0.017	0.42	0.00425	1
Load tube	0.017	2	0.00425	1

where p_r is the oscillating pressure, and U_r is the oscillating volume flow rate. A_r and l_r are the cross-sectional area and length of regenerator, respectively. p_m, ρ_m, T_m, l, γ, Pr and Sc are the mean pressure, mean density, mean temperature, latent heat, specific heat ratio, Prandtl number and Schmidt number of working fluid, respectively. n_g is the number density (i.e., the number of particles per unit volume [9]) of gas working fluid and n_w is the number density of liquid working fluid. f_v, f_κ and f_D are the viscous function, thermal function and mass diffusion function, respectively. ω is the angular frequency and i is the imaginary unit. R_0 is the gas constant.

From the viewpoint of acoustic-electric analogy [12], the oscillating pressure difference (p) and volume flow rate (U) are taken as the voltage difference (E) and current (I), respectively. Hence, Equations (4) and (5) can be rewritten into the following forms:

$$\Delta p_r = -(R_v + i\omega L_v)U_r \quad (6)$$

$$\Delta U_r = -(\frac{1}{R_\kappa} + i\omega C_\kappa)p_r + G_r U_r \quad (7)$$

Accordingly, the equivalent viscous resistance R_v, inductance L_v, thermal-relaxation resistance R_κ, capacitance C_κ and controlled source G_r can be expressed as:

$$R_v = \frac{\omega \rho_m l_r}{A_r} \frac{\mathrm{Im}[-f_v]}{|1-f_v|^2} \quad (8)$$

$$L_v = \frac{\rho_m l_r}{A_r} \frac{1-\mathrm{Re}[f_v]}{|1-f_v|^2} \quad (9)$$

$$\frac{1}{R_\kappa} = \frac{\omega A_r l_r}{P_m}\left\{\frac{\gamma-1}{\gamma}\mathrm{Im}[-f_\kappa] + \frac{n_w}{n_g}\mathrm{Im}[-f_D]\right\} \quad (10)$$

$$C_\kappa = \frac{A_r l_r}{\gamma P_m}\left\{1 + (\gamma-1)\mathrm{Re}[f_\kappa] + \frac{n_w}{n_g}\gamma\,\mathrm{Re}[f_D]\right\} \quad (11)$$

$$G_r = \left\{\frac{(f_\kappa - f_v)}{(1-f_v)(1-\mathrm{Pr})} + \frac{l}{R_0 T_m}\frac{n_w}{n_g}\frac{(f_D - f_v)}{(1-f_v)(1-\mathrm{Sc})}\right\}\frac{dT_m}{T_m} \quad (12)$$

Except for the regenerator, all other components in the modified two-phase thermofluidic oscillator follow the definitions of Markides and Smith [5]. The detailed formulation of the acoustic-electric analogy elements and their impedances can be referred in the works of Markides and Smith [5] and Tan et al. [9, 10].

IV. RESULTS AND DISCUSSION

To validate the acoustic-electric analogy model, the frequency and onset temperature difference of the modified two-phase thermofluidic oscillator with R152a and R1234yf are experimentally examined. Table II lists the specific heat ratio, Prandtl number, ozone depletion potential (ODP) and global warming potential (GWP) of R152a, R1234yf and R1234ze(E) at the temperatures of 22°C. Then, the effects of the lengths and diameters of feedback connection tube and vapor connection tube on the performance are numerically studied.

A. Experimental validation

Fig. 3 illustrates the predicted oscillation frequencies with different liquid column lengths inside the load tube, if R152a and R1234yf are adopted as working fluids. Besides, the experimental results of oscillation frequency are presented for model validation. The oscillation frequency reduces when enlarging the liquid column length. Additionally, the calculated oscillation frequencies agree well with the experimental results. The differences between the predicted and measured oscillation frequencies are in the range of 4.4-6.8%, which are mainly attributed to the neglect of the variation in pressure induced by the increased working fluid temperature. An enlarged liquid column length results in the increased inductance, and thus causes a reduction in the oscillation frequency. The working fluids with different specific heat ratios will affect the oscillation frequency. The system with R152a obtains higher oscillation frequency because R152a has larger specific heat ratio than R1234yf. The highest oscillation frequency obtained is 2.95 Hz with R152a as working fluid.

Fig. 3 also presents the experimental and computed onset temperature differences when adjusting the liquid column length inside the load tube. The onset temperature difference rises with the liquid column length. The calculated onset temperature differences are in reasonable agreement with the experiments, with the errors of 5.4-13.4%. The deviations can mainly be attributed to the neglect of the dissipated acoustic power caused by the variation in cross-section area. An increased liquid column length brings about the increased viscous loss, and then causes an elevation in the onset temperature difference. As listed in Table II, the Prandtl number of R1234yf is smaller than that of R152a. Therefore, the onset temperature difference with R1234yf as working fluid is lower than that with R152a.

TABLE II. SPECIFIC HEAT RATIO, PRANDTL NUMBER, ODP AND GWP OF THREE WORKING FLUIDS (AT 22°C).

Working fluid	Specific heat ratio	Prandtl number	ODP	GWP
R152a	1.2579	0.8496	0	138
R1234yf	1.1949	0.8361	0	<1
R1234ze(E)	1.1612	0.8741	0	<1

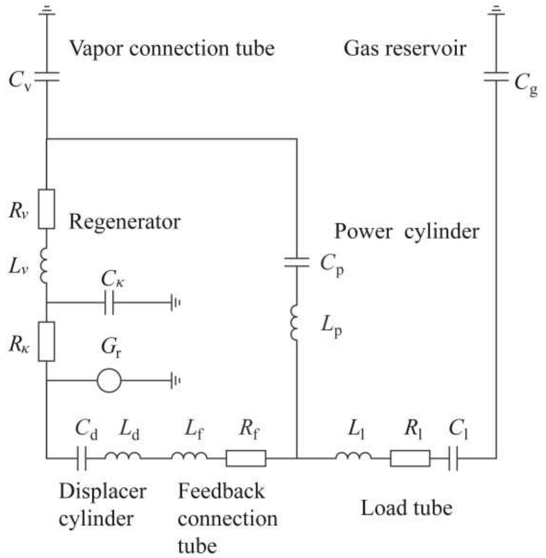

Fig. 2. Acoustic-electric analogy circuit of the modified two-phase thermofluidic oscillator

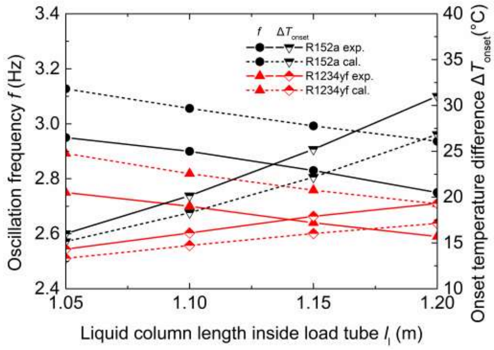

Fig. 3. Oscillation frequency and onset temperature difference versus liquid column length inside the load tube

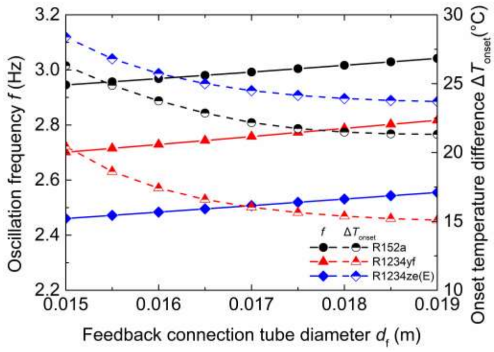

Fig. 4. Oscillation frequency and onset temperature difference versus feedback connection tube diameter

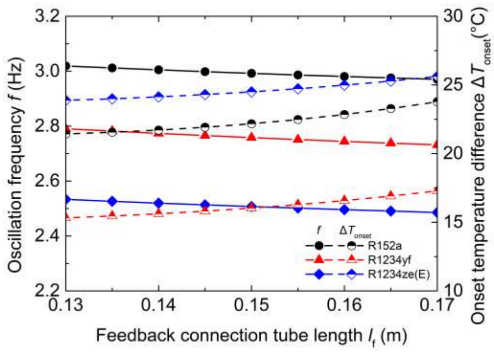

Fig. 5. Oscillation frequency and onset temperature difference versus feedback connection tube length

B. Parametric study

Two connection tubes (i.e., feedback connection tube and vapor connection tube) play a vital role in the distribution of acoustic field in the looped structure, which largely affect the onset characteristics. The influences of the lengths and diameters of feedback connection tube and vapor connection tube on the frequency and onset temperature difference are numerically studied, with all other parameters kept at their initial values (Table I). The liquid column length inside the load tube is 1.15 m. Except for R152a and R1234yf, R1234ze(E) with ODP of 0 and GWP of 1 is also used as working fluid.

Fig. 4 shows the resonant frequency and onset temperature difference with respect to feedback connection tube diameter. The oscillation frequency increases when the feedback connection tube diameter is increased. An increased feedback connection tube diameter can lead to a reduction in its inductance, which then brings about an increase in the oscillation frequency. Besides, the oscillation frequency is found in the increasing order of R1234ze(E), R1234yf and R152a. The highest oscillation frequency of 3.04 Hz can be obtained with R152a as working fluid, when the feedback connection tube diameter is 0.019 m.

The onset temperature difference decreases with the feedback connection tube diameter, whose rise can result in a reduction in its resistance. As listed in Table II, the Prandtl number is in an increasing order of R1234yf, R152a and R1234ze(E). Hence, the onset temperature difference with R1234yf is the lowest, then R152a and finally R1234ze(E).

Fig. 5 presents the effect of feedback connection tube length on frequency and onset temperature difference. Lengthening the feedback connection tube causes a slight reduction in the resonant frequency. When using R152a as working fluid, an increase in the feedback connection tube length from 0.13 m to 0.17 m can bring about a reduction in the frequency from 3.02 Hz to 2.97 Hz. Increasing the feedback connection tube length can lead to a rise in its inductance, which then causes a reduction in the oscillation frequency. Additionally, an increased feedback connection tube length leads to an increase in its resistance, and thus results in an elevation in the onset temperature difference.

The oscillation frequency and onset temperature difference with respect to vapor connection tube diameter are shown in Fig. 6. The oscillation frequency is less sensitive to the vapor connection tube diameter. The slight decrease is mainly ascribed to the increased capacitance induced by an increase in the vapor connection tube diameter. In addition, the onset temperature difference rises with the vapor connection tube diameter when adopting R152a and R1234yf as working fluids. However, the vapor connection tube length has almost no impact on the onset temperature difference with R1234ze(E) as working fluid. Among three working fluids, a lowest onset temperature difference of 14.4°C can be obtained with R1234yf as working fluid, when the vapor connection tube diameter is 0.015 m.

Fig. 7 illustrates the resonant frequency and onset temperature difference as functions of vapor connection tube length. The oscillation frequency varies little with the vapor connection tube length. An increase in the vapor connection tube length from 0.4 m to 0.44 m leads to a slight reduction in the frequency, less than 0.02 Hz for all three working fluids. Similarly, the onset temperature difference is not sensitive to the variation of vapor connection tube length. An increase in the vapor connection tube length from 0.4 m to 0.44 m only induces a rise less than 0.8°C in the onset temperature difference for all three working fluids.

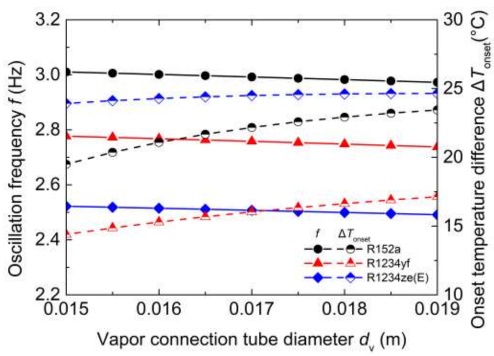

Fig. 6. Oscillation frequency and onset temperature difference versus vapor connection tube diameter

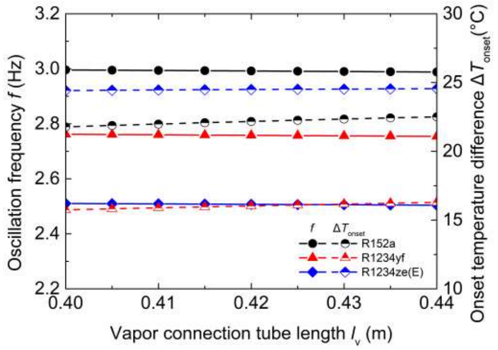

Fig. 7. Oscillation frequency and onset temperature difference versus vapor connection tube length

V. Conclusions

The performance of a modified two-phase thermofluidic oscillator with low GWP working fluids is studied. An acoustic-electric analogy model is proposed for predicting its onset temperature difference and frequency, and is then experimentally validated. The influences of the lengths and diameters of feedback connection tube and vapor connection tube on the performance are numerically examined. The main conclusions are summarized as follows:

(1) The acoustic-electric analogy model can well predict the oscillation frequency, with the differences of 4.4-6.8% from experimental results. Besides, the predicted and measured onset temperature differences are in reasonable agreement, since the proposed model underestimates the experimental onset temperature differences by 5.4-13.4%.

(2) Working fluid has a marked effect on the onset features. The oscillation frequency with R152a as working fluid is the highest thanks to its largest specific heat ratio. The system with R1234yf obtains the lowest onset temperature difference, owing to its lowest Prandtl number.

(3) Upon optimization, a highest oscillation frequency achieved is 3.04 Hz with R152a as working fluid, when the feedback connection tube diameter is increased to 0.019 m. Besides, a lowest onset temperature difference of 14.4℃ can be obtained with the vapor connection tube diameter of 0.015 m, when using R1234yf as working fluid.

Acknowledgment

This work is financially supported by the Natural Science Foundation of Zhejiang Province (LZ20E060004) and the National Natural Science Foundation of China (51576170).

References

[1] Intergovernmental Panel on Climate Change, "Special Report on Global Warming of 1.5°C," Cambridge: Cambridge University Press, 2018.

[2] S. Brückner, S. Liu, L. Miró, M. Radspieler, L. F. Cabeza, E. Lävemann, "Industrial waste heat recovery technologies: An economic analysis of heat transformation technologies," Appl. Energy London, vol. 151, pp. 157–167, 2015.

[3] W. Qu, H. Hong, B. Su, S. Tang, H. Jin, "A concentrating photovoltaic/Kalina cycle coupled with absorption chiller," Appl. Energy London, vol. 224, pp. 481–493, 2018.

[4] J. Tan, J. Luo, Y. Wang, J. Wei, T. Jin, "Performance of an air-cooled looped thermoacoustic engine capable of recovering low-grade thermal energy," Int. J. Energy Res. New Jersey, Doi: 10.1002/er.5034

[5] C. N. Markides, T. C. B. Smith, "A dynamic model for the efficiency optimization of an oscillatory low grade heat engine," Energy London, vol. 36, pp. 6967–6980, 2011.

[6] A. I. Taleb, M. A. G. Timmer, M. Y. El-Shazly, A. Samoilov, V. A. Kirillov, C. N. Markides, "A single-reciprocating-piston two-phase thermofluidic prime-mover," Energy London, vol. 104, pp. 250–265, 2016.

[7] M. Glushenkov, M. Sprenkeler, A. Kronberg, V. Kirillov, "Single-piston alternative to Stirling engines," Appl. Energy London, vol. 97, pp. 743–748, 2012.

[8] C. J. W. Kirmse, O. A. Oyewunmi, A. I. Taleb, A. J. Haslam, C. N. Markides, "A two-phase single-reciprocating-piston heat conversion engine: Non-linear dynamic modelling," Appl. Energy London, vol. 186, pp. 359–375, 2017.

[9] J. Tan, J. Wei, T. Jin, "Electrical-analogy network model of a modified two-phase thermofluidic oscillator with regenerator for low-grade heat recovery," Appl. Energy London, vol. 262, pp. 114539, 2020

[10] J. Tan, J. Wei, T. Jin, "Onset and damping characteristics of a closed two-phase thermoacoustic engine," Appl. Therm. Eng. London, vol. 160, pp. 114086, 2019.

[11] J. R. Taylor, "An introduction to error analysis: the study of uncertainties in physical measurements," New York: University Science Books, 1997.

[12] G. W. Swift, "Thermoacoustics: a unifying perspective for some engines and refrigerators," New York: American Institute of Physics Press, 2002.

[13] R. Raspet, W. V. Slaton, C. J. Hickey, R. A. Hiller, "Theory of inert gas-condensing vapor thermoacoustics: Propagation equation," J. Acoust. Soc. Am. New York, vol. 112, pp. 1412–1422, 2002.